HHS Public Access

Author manuscript

Trends Biochem Sci. Author manuscript; available in PMC 2016 November 01.

Published in final edited form as:

Trends Biochem Sci. 2015 November ; 40(11): 648–661. doi:10.1016/j.tibs.2015.09.001.

Chemistry and biology of self-cleaving ribozymes

Randi M. Jimenez[1], **Julio A. Polanco**[1], and **Andrej Lupták**[2]

[1]Department of Molecular Biology and Biochemistry, University of California, Irvine, California, USA

[2] Departments of Pharmaceutical Sciences, Chemistry, and Molecular Biology and Biochemistry, University of California, Irvine, California, USA

Abstract

Self-cleaving ribozymes were discovered thirty years ago, but their biological distribution and catalytic mechanisms are only beginning to be defined. Each ribozyme family is defined by a distinct structure with unique active sites accelerating the same transesterification reaction across the families. Biochemical studies show that general acid-base catalysis is the most common mechanism of self-cleavage, but metal ions and metabolites can be employed as cofactors. Ribozymes have been discovered in highly diverse genomic contexts throughout nature, from viroids to vertebrates. Their biological roles include self-scission during rolling-circle replication of RNA genomes, co-transcriptional processing of retrotransposons, and metabolite-dependent gene expression regulation in bacteria. Other examples, including highly conserved mammalian ribozymes, suggest that many new biological roles are yet to be discovered.

Keywords

ribozyme; riboswitch; retrotransposon; aptazyme; self-scission; riboregulation

Guiding principles for ribozyme exploration

Small nucleolytic ribozymes carry out site-specific phosphodiester scission without the need for protein chaperones or enzymes. A growing number of ribozyme families are found in nature, including: hairpin, hammerhead, **hepatitis delta virus (HDV)-like**, ***glmS***, *Neurospora* Varkud satellite, twister, the recently discovered twister sister, pistol, and hatchet motifs. All rely on a combination of catalytic strategies to complete self-scission in an active site formed by the secondary and tertiary structures unique to each family. For these ribozymes, cleavage involves a nucleophilic attack by a 2′ oxygen on an adjacent phosphodiester bond, yielding a 2′-3′ cyclic phosphate and a 5′-hydroxyl product (Fig. 1). Crystal structures have been essential to illuminate how functional groups participate in the catalytic mechanism used by each family of ribozyme. The local electronic environments

aluptak@uci.edu..

within the active sites shift pK_a values, allowing nucleobases and cofactors to participate in general acid-base catalysis. Despite the plethora of information regarding their genomic distributions, structures, and mechanisms, the biological roles of the three most widespread families (hammerhead, HDV-like, and twister) remain largely elusive. The study of small ribozymes has provided a platform for discovering new catalytic RNAs and new roles for **non-coding RNA (ncRNA)**, as well as aided in the design of new molecules for synthetic biology. Here, we summarize the recent mechanistic findings of the six best-described types of self-cleaving ribozymes and discuss their potential impact on the surrounding transcripts. The discovery of three new types of self-cleaving ribozymes earlier this year (2015) suggests that there are more catalytic RNAs with new biological functions to be uncovered.

Hepatitis delta virus family of ribozymes

The HDV life cycle depends on coinfection with hepatitis B virus (HBV) [1] and it relies on host cellular machinery for rolling-circle replication of its single-stranded RNA genome (Fig. 2A) [2]. The HDV genome encodes two related but distinct ribozymes that were first discovered through their function in processing concatameric copies of the viral RNA genome during rolling circle transcription (Fig. 2A) [3]. More recently, this ribozyme motif was discovered in the human genome using *in vitro* selection from a genomic library; sequence analysis showed that it is highly conserved in mammals [4]. When its nested double-pseudoknot secondary structure was used to identify the motif in other genomes (Box 1), the family of HDV-like ribozymes was found to exist in nearly all branches of life [5]. These HDV-like ribozymes often map to the 5′ **UTR** of autonomous (**LINE**) retrotransposons, pointing to a role in the processing of retrotransposons (Fig. 2B). Expression analysis and 5′ processing studies support a model in which HDV-like ribozymes function at several stages of in non-**long terminal repeat** (non-LTR) retrotransposition [6-8]. Besides processing the 5′ end of the transposon RNA out of the parent transcript, ribozymes may be promoting the translation of the open reading frame of the retroelement [5], and facilitating the insertion of the retrotransposon into a new DNA locus. In support of this idea an RNA 5′-hydroxyl, such as would result from ribozyme self-cleavage, increases efficiency the of R2 reverse transcriptase template switching, completing the R2 LINE retrotransposition cycle [9, 10].

Further biological roles of these ribozymes suggest that their activity (1) is regulated, (2) affects the surrounding transcript and, remarkably, (3) is associated with a phenotype in humans. In the mosquito *Anopheles gambiae* expression and self-scission analyses revealed that both the *in vivo* levels and the extent of self-cleavage varies by sex and life stage [5], suggesting environmental sensitivity and regulation. The HDV-like ribozyme found in an intron of the cytoplasmic polyadenylation element binding protein 3 (*CPEB3*) gene is highly conserved in mammals [4], and people homozygous for a **single nucleotide polymorphism (SNP)** known to affect *CPEB3* ribozyme activity show differences in episodic memory [11]. Other HDV-like ribozymes are located at unrelated genomic loci in both coding and non-coding transcripts, suggesting multiple biological functions. HDV-like ribozymes have fast self-cleavage kinetics and have a remarkably stable structure, demonstrating activity in up to 18 M formamide [12, 13], therefore some of the cellular functions may be related to

stabilizing the 5′ termini of the cleaved transcripts and protecting them from degradation by exonucleases.

The HDV ribozyme secondary structure is composed of five helical regions (P1.1, P1, P2, P3, P4) forming two coaxial stacks (P1, P1.1 stack on P4 and P2 stacks on P3) that are joined by single stranded regions (J1/2, L3, J4/2) (Fig. 3A). There are six conserved nucleotides fulfilling functional or structural roles in the active site. The ribozyme exists naturally in a minimal (lacking P4) or extended (extension of J1/2 and P4) form. Crystal structures of the genomic HDV ribozymes revealed that the secondary structure forms a nested double-pseudoknot (Fig. 3A) and the active site is buried in the junction of P1, P1.1 and P3 [14-16]. The protonated form of C_{75} is thought to be stabilized through interactions with the scissile phosphate [16] and may interact electrostatically with the metal ion bound in the active site [17]. Divalent metals have a profound impact on catalysis and recent evidence reveals a Mg^{2+} ion in a metal binding pocket in the ribozyme active site [16, 18].

The proposed mechanism of catalysis suggests that HDV ribozymes are multi-channel, employing different strategies in the presence and absence of divalent metal ions. In one scenario, the protonated form of C_{75} donates a proton to the 5′-O of G_1 [19]. The HDV-like ribozymes are metalloenzymes under biological conditions with the divalent metal cation thought to stabilize the developing negative charge on the 2′ nucleophile [18], facilitating deprotonation by a general base, likely a hydroxide ion, and also potentially stabilizes the pentavalent phosphorane transition state [20]. There is little metal ion specificity and catalysis can proceed in high concentrations of monovalent cations alone [21]. In the absence of divalent cations, the dramatic shift in pK_a of the catalytic nucleobase C_{75} may be sufficient to stabilize the negatively charged nucleophile and general acid-base catalysis proceeds without mediation by a divalent metal cation [22, 23]. Even though HDV ribozymes were the first to have general acid-base mechanism proposed [20], efficient catalysis by HDV and HDV-like ribozymes appears to require both a divalent metal ion and an active-site cytosine acting as a general acid (Table 1). This mechanism turns out to be unique among natural self-cleaving ribozymes, as the other motifs described in this review all appear to only use nucleotides for catalysis (Table 1).

Hammerhead ribozyme

The hammerhead ribozyme (HHR) was originally discovered in **viroids** and **virusoids** where it functions in the processing of rolling-circle transcripts (Fig. 2A) [24-26]. Over the next two decades, isolated instances were found in various newt species [27], cave crickets [28], and the human blood fluke *Schistosoma mansoni* [29]. HHRs found in the genomes of various schistosomes map to **short interspersed element-like (SINE)** retrotransposable elements (Fig. 2C) [29, 30]. The conservation of these SINE-associated HHRs suggests vertical transmission from a common ancestor of schistosomes. The HHR is perhaps the most widespread ribozyme family, having been found across all domains of life [27-29, 31-35]. Most eukaryotic occurrences map to satellite transcripts and retroelements; however, a conserved group in amniotes map to the introns of specific genes [32, 33, 36]. This conservation in introns implicates a role for these ribozymes in pre-mRNA processing. The ribozyme has also been found bisected into two fragments hundreds of nucleotides apart

between the stop codon and the polyadenylation signal of mouse C-type lectin type II (*Clec2*) and some mammalian *Clec2-like* genes [37]. It seems that the mechanism of ribozyme phosphodiester scission may have been adapted to introduce diversity in gene expression and more complex genetic controls, but more research is needed to decipher the potential role of HHRs in intron cleavage and pre-mRNA processing. The efficient self-scission of HHRs *in vitro* and *in vivo* suggests the activity is central to their biological significance.

The HHR secondary structure is comprised of three helices (stems I, II, III) branching from a catalytic core containing fifteen nucleotides essential to catalysis (Fig. 3B). The ribozyme exists naturally in three circularly permuted topologies (types I, II, and III), defined by the helix connecting it to the surrounding transcript (Box 1). The HHR was the first ribozyme to have its crystal structure solved [38, 39] revealing the core trapped in an open or pre-catalytic state that would require significant rearrangement to bring the essential residues into position for in-line attack. Subsequent mechanistic and structural data conflicted until the discovery of a distal tertiary contact (between stems I and II) [40, 41], which promotes significantly faster cleavage rates, presumably because it stabilizes the catalytically competent conformation of the active site. The global structure of the ribozyme is Y-shaped, comprising a coaxial stack of stems III and II that pack next to stem I (Fig. 3B), optimally positioning residues implicated in general acid-base catalysis, and for the nucleophile to attack the scissile phosphate [42].

The currently proposed model of catalysis by a HHR involves only nucleotides participating directly in catalysis. Biochemical and crystallographic evidence supports C_{17} nucleophilic attack on the adjacent scissile phosphate of $C_{1.1}$. Invariant residues G_8 and G_{12} serve as a general acid and a general base, respectively [43]. A recent crystal structure revealed three Na^+ cations in the HHR active site, one of which binds to G_{12} and may be involved in stabilizing the negative charge of the deprotonated N1 position [44]. A role for monovalents in perturbing the pK_a of the general base had been suggested previously [45, 46]. The N1 of the ionized form of G_{12} is thought to abstract the 2′ hydrogen from the nucleophilic oxygen of C_{17}, the 2′-O is then positioned for in-line attack on the phosphate of $C_{1.1}$ (Fig. 3B) [47]. The ribose of G_8 likely hydrogen-bonds to the 5′-oxyanion and donates a proton to the leaving group [42, 47, 48]. The proposed mechanism is unique in that it employs a nucleobase and a ribose, a composition that may be easier to bring into the active site than two nucleobases or exogenous cofactor, and may contribute to the high frequency with which this self-cleaving ribozyme is found in nature.

Hairpin ribozyme

There are only three known examples of the hairpin ribozyme family, residing in the satellite RNAs of the tobacco ringspot [24], chicory yellow mottle [49], and arabis mosaic viruses [50]. Each occurrence coincides with the appearance of a HHR on the RNA of opposite strand and together these ribozymes function in processing multimeric RNA during rolling circle replication of the viral genome (one on the + strand and one on the – strand). The hairpin ribozyme secondary structure is composed of four helical stems (A-D) anchored in a four-way junction and forming two coaxial stacks (D stacks on A and C stacks on B) (Fig.

3C). Stems A and B contain internal bulges housing the scissile phosphate (stem A) and nucleotides essential to catalysis, whereas stems C and D provide structural stability and are not necessary for ribozyme activity.

Crystal structures of the hairpin ribozyme have been determined with and without stems C and D, the junction [51] and hinge forms [52], respectively. The structures support biochemical evidence for the intimate interaction of loops A and B, which form the active site of the ribozyme (Fig. 3C) [51-53]. A_{38} and G_8 are optimally positioned to serve as general acid and general base, respectively. G_8 is on the strand opposite of the scissile phosphate in loop A and A_{38} is in loop B. Single molecule studies revealed that the loop-loop interaction is dynamic and oscillates between an antiparallel (active form) and parallel states [54, 55].

The highly stabilized extrusion of G_{+1} constrains the riboses of A_{-1} and G_{+1},respectively the nucleotides upstream and downstream of the cleavage site, enabling the in-line arrangement of the nucleophile and leaving group [52]. The crystal structure of hairpin enzymes with vanadate, a transition state mimic, points to a role for A_{38} and G_8 as general acid and general base, as well as transition state stabilization by binding the *pro-R* and *pro-S* oxygens of the scissile phosphate, respectively [53]. These roles are supported by functional group modifications and nucleobase substitution experiments [56-59] and appear to exemplify the most general theme in self-scission mechanisms (Table 1).

Neurospora Varkud satellite ribozyme

The Varkud satellite (VS) ribozyme is important in replication of a single-stranded RNA satellite found in some strains of *Neurospora* [60]. The secondary structure of the VS ribozyme is composed of seven helices (I-VII) that form three three-way junctions (Fig. 3D). A kissing loop interaction between stem-loops I and V [61] facilitates docking of the internal loop of stem I with the internal loop of stem VI which forms the active site. First predicted based on site-directed mutagenesis and chemical modification analysis [62, 63], the interaction involves a conformational change (shift) in SLI that is necessary for ribozyme activity [64-66]. The SLI-SLV interaction facilitates the docking of SLI with SLVI thereby forming the active site [65, 67, 68]. The SLI/SLV kissing loop NMR structure has been solved [69-71] and supporting isothermal titration calorimetry experiments demonstrate that the SLI/SLV kissing-loop interaction is a major thermodynamic barrier and is therefore likely regulating ribozyme activity [61]. The formation of the SLI/SLV interaction relies upon divalent metal cations; however, there is no evidence for their direct involvement in catalysis.

There is currently no crystal structure solved for the VS ribozyme, however X-ray scattering experiments reveal A_{756} (stem loop VI) and G_{638} (stem loop I) are positioned in close proximity to the scissile phosphate [72]. Biochemical evidence suggests that A_{756} acts as the general acid and G_{638} as the general base during self-scission [73, 74], similarly to the mechanism proposed for the hairpin ribozyme wherein a guanosine and adenosine facilitate general acid-base catalysis (Table 1).

Glucosamine 6-phosphate synthase (*glmS*) ribozyme

The *glmS* ribozyme was discovered as a conserved motif located in the 5′ UTR of the *glmS* gene, encoding glutamine-fructose-6-phosphate amidotransferase, in many Gram-positive bacteria [75]. It is the only example of a metabolite-responsive self-cleaving ribozyme, utilizing glucosamine 6-phosphate (glcN6P) as a cofactor necessary for catalysis. It is also a riboswitch, regulating the expression of the *glmS* gene by a negative feedback mechanism whereby scission of the mRNA results in degradation of the message and a decrease in synthesis of the enzyme generating the glcN6P. Self-cleavage is completely dependent on the presence of amine-containing ligands, and the pK_a of the amine functionality impacts reactivity but not binding affinity [76].

The structure of the *glmS* ribozyme is composed of three coaxial stacks (P1 stacks P3.1, P4 stacks P4.1, and P2.1), which are packed in a nearly parallel fashion (Fig. 3E). The core of the ribozyme is doubly pseudoknotted (P2.1 and P2.2 are pseudoknots). P2.2 contains the scissile phosphate and helps to form the binding site for the glcN6P cofactor. P3 and P4 are not necessary for activity; however, they enhance cleavage by providing structural stability [75, 77]. Crystal structures of both pre- and post-cleavage states showed no significant conformational change upon ligand binding [78]. The crystal structures revealed the location of a divalent metal, the metabolite binding pocket, and the active site, and provided strong evidence for the role of glcN6P in the catalytic mechanism. Both glcN6P [79, 80] and the competitive inhibitor glc6P [78] are buried in the metabolite binding pocket, and both the sugar and phosphate of the cofactor are recognized in the pocket: the G_1 nucleobase stacks on the sugar ring, and N1 H-bonds to the phosphate, which also coordinates a Mg^{2+} cation. The 1-hydroxyl of glc6P donates an H-bond to the pro-*R*p oxygen of the scissile phosphate A_{-1} and accepts a H-bond from N1 of G_{65} (Fig. 3E; numbering follows that of the ribozyme used in the crystal structure from ref. [78]). The 2-OH of glc6P forms a H-bond to the 5′-O of G_1 [78], whereas in the presence of glcN6P, the amine moiety makes the interaction, making it a strong candidate for general acid during catalysis [79].

At the active site, G_{65} forms an irregular base pair with A_{-1}. Together, G_{39} and G_{65} position the scissile phosphate by binding its non-bridging oxygens. These interactions, along with the 2′-endo ribose pucker of A_{-1}, twist the RNA backbone into a nearly perfect in-line conformation. The nucleotides 5′ and 3′ of the scissile phosphate are unstacked and splayed apart. Overall, the active site is remarkably rigid, perhaps explaining why the *glmS* ribozyme is the only ribozyme besides the ribosome to be active in the crystallized form.

G_{40} and the metabolite are ideally positioned to serve as general base and acid, respectively, in catalysis (Fig. 3E). Raman crystallography revealed the ionization states of the glcN6P cofactor and supports the role of G_{40} in tuning the pK_a of both the phosphate and amine of the ligand [81]. This is remarkable considering the amine of free glcN6P is neutral. Thus, the positively charged amine is positioned to serve in proton transfer. The relationship between the ionization state of the cofactor and the ribozyme activity support the role of the cofactor in proton transfer [82]; however, the only evidence for the respective roles of G_{40} and the glcN6P cofactor in catalysis are their positions within the active site. Further analyses of this riboswitch-ribozyme will help define the details of it catalytic mechanism.

Twister ribozyme

The twister ribozyme was discovered in 2013 through bioinformatics searches for conserved RNA structural motifs [83]. The secondary structure is composed of three stems (P1, P2, P4) joined by internal and terminal loops (L1, L2, L4). There are two pseudoknots: PK2 is formed between L1 and L4, PK1 formed by L2 and L4 (Fig. 3F; the numbering convention follows that of ref [83]). The ribozyme can exist in an extended format with additional stem loops P3 and P5 creating a three- or four-way junction at L2. In addition, the twister ribozyme can exist in three circularly permuted varieties (P1, P3, or P5). Twister ribozymes demonstrate robust cleavage kinetics both *in vitro* ($k_{obs} > 1\ min^{-1}$ at physiological conditions) and *in vivo* [83]. Biochemical and crystallographic evidence support the roles of ten conserved nucleotides at the active site.

The crystal structure of the *Oryza sativa* (Osa-1-4) P1 type twister ribozyme lacking P3 and P5 was solved to 2.3 Å resolution [84]. The structure correlates well with that predicted by covariation and in-line probing analysis [83]. Helices P1, PK1(T2), P2, and PK2(T1) are coaxially stacked and P4 lies approximately parallel to the stack. The active site is located in the major groove of the PK2(T1)-P2 helix. G_{45} donates a hydrogen-bond to the *proR*-O of the scissile phosphate of A7 (in P1) and has been proposed to transfer the 2′ proton during catalysis [84]. Although there is no direct biochemical evidence, modeling based on the crystal structure points to a possible role of A_7 in the catalytic mechanism (Fig. 3F) [84]. Another crystal structure of a P1-type twister identified in a metagenomic sequence revealed a Mg^{2+} ion near the scissile phosphate [85]. As in many other ribozyme active sites, the nucleotides flanking the scissile phosphate are splayed apart, promoting the in-line arrangement necessary for catalysis. The resolution of a divalent cation along with the ordering and in-line arrangement of the U_6 nucleophile and A_7 leaving group is unique to this study and provides further elucidation of the factors contributing to the remarkable rates of catalysis by twister ribozymes.

Two additional crystal structures of type-P3 twister ribozymes from *O. sativa* and an environmental (metagenomic) sequence further suggest that a conserved adenosine is involved in stabilizing the negative charge on a non-bridging oxygen at the cleavage site, in addition to a guanosine activating the nucleophile [86]. The twister crystal structures suggest the utilization of a transition state stabilization strategy similar to the hairpin ribozyme. Remarkably, the source of protons for the 5′ oxyanion leaving group remains unknown (Table 1); however, crystallization of a transition state analog of the ribozyme may yet reveal a new active site rearrangement and clearly defined proton donor.

Mechanistic conclusions

What have we learned so far? As Table 1 shows, the common theme in ribozyme-self-scission is general acid-base catalysis. Ribozymes were originally thought to be metalloenzymes, in which the RNA serves to position catalytic Mg^{2+} ions to accelerate phosphoryl transfer [87, 88]. The small self-cleaving ribozymes described here have evolved catalytic mechanisms mostly independent of metal ions and the origin of this mechanistic separation is unknown. A notable distinction between the two groups of phosphotransferases

is that the self-cleavers act just once, whereas the larger ribozymes act twice (in case of self-splicing introns) or more (in case of the spliceosome and RNase P). Some of these small ribozymes represent the simplest evolutionary solution, as *in vitro* selections suggest [89], and general acid-base catalysis is perhaps the simpler mechanistic solution to RNA self-scission.

Biological significance

Self-cleaving ribozymes are remarkably efficient enzymes, and we are continuing to discover their importance in biological systems. The biology of these common ribozymes remains one of the most unexplored areas of RNA research. The *glmS* ribozyme is unique in its role as a riboswitch controlling the flux of glcN6P in many Gram-positive bacteria. For the hairpin and VS ribozymes, each known instance is associated with a defined biological role in viral genome replication, although their true distribution may reach further than we currently understand. The HHR, HDV-like, and twister ribozyme families are widespread and found in diverse biological contexts, but only few isolated occurrences have been studied for their particular influence on genetic controls [6, 36].

The presence of self-cleaving ribozymes in intronic regions presents an exciting avenue of research with relevance to pre-mRNA processing and alternative splicing. Multiple HHRs are found in introns of a conserved set of genes in amniotes [32] and the ultraconserved HDV-like ribozyme mapping to the *CPEB3* gene in mammals is also located in an intron [4]. For the *CPEB3* and R2 retrotransposon-associated HDV-like ribozymes, RT-qPCR analyses demonstrate that the levels of cleaved product vary by tissue or life-stage, respectively [4, 5]. These observations suggest that the catalytic activity of these ribozymes is regulated, lending additional support to the idea that ribozymes are presenting an additional level of control for the expression of genes in which they reside. Interestingly, engineering self-cleaving ribozymes into introns or exons is a strategy used to understand co-transcriptional pre-mRNA processing [90]. These studies use a kinetic competition between splicing and ribozyme self-cleavage, the latter of which is disruptive to splicing [91] if ribozyme catalytic rates are “fast” enough so as to interfere with spliceosome assembly [90].

In some natural cases, multiple ribozymes are found near each other in the same genomic locus [5, 31, 83], suggesting a cooperative influence on transcript processing or function. For example, some eukaryotic HHRs that are found associated with **Penelope-like elements (PLEs)**, a family of retrotransposons, display an organization suggestive of dimerization [92]. The dimeric form, containing two sites of self-cleavage, is possible when HHRs occur in tandem and has been shown to lead to a more stable active structure compared to monomeric species of the ribozyme [93]. By contrast, the discontinuous HHR present in the 3′ UTR of rodent *Clec2* genes is a single HHR in which invariant regions comprising the ribozyme core are separated by hundreds of nucleotides. The self-cleavage activity of this *Clec2* HHR removes the polyadenylation signal from the 3′ end of the mRNA, leading to a reduction in protein expression *in vivo* [37].

Very few known self-cleaving ribozymes are highly conserved amongst eukaryotic genomes. In rare instances, such as the *Clec2*-associated HHRs and the *CPEB3* HDV-like ribozymes, a single ribozyme sequence is conserved across multiple organisms [4, 37], demonstrating that the self-scission activity was preserved through evolutionary lineages. On the other hand, many instances of HHR, HDV-like, and twister ribozymes are found associated with mobile genetic elements and are thus not well conserved in terms of genetic loci or even sequence [5, 92, 94]. The extensive distribution of these ribozymes suggests they are common genomic features, perhaps distributed via (sub-)viral elements, retrotransposons and other repeats, but now associated with multiple biological functions. While the field has gained a wealth of knowledge from studying independent examples of genetic elements harboring self-cleaving ribozymes, the biological significance of many other instances remains elusive.

The discovery of new self-cleaving ribozymes has transitioned from uncovering autocatalysis by single transcripts to high throughput bioinformatic approaches to identifying conserved RNA structures. As the power of computational and high-throughput RNA structure probing methods continues to grow, undoubtedly new complex and intricate RNA motifs will be revealed, among them possibly new families of self-cleaving ribozymes. In fact, recent computational searches have uncovered structural variants of known ribozymes and discovered new conserved RNA motifs in bacterial genomes. Three new families of ribozymes have been validated for self-cleavage activity *in vitro*: twister sister, hatchet, and pistol [95]. These new ribozyme families provide the opportunity to gain insight to the biochemical capacity of structured RNAs and gain further understanding for the biological significance of self-cleaving ribozymes.

In vitro selections from genomic and synthetic DNA pools suggest that there are other motifs in nature capable of catalyzing self-scission and its reverse, ligation [4, 89, 96]. In addition, ribozyme catalysis can be studied in a trans-cleaving format, where the bisection of secondary structure allows substrate recognition to regulate the rate of catalysis. The ease with which robust *trans*-cleaving ribozymes can be designed and constructed suggests that these intermolecular interactions might also exist in nature. Similar to ribozymes, riboswitches are typically *cis*-acting, controlling transcription, translation, or stability of the proximal mRNA. Interestingly, an S-adenosyl methionine riboswitch element in the genome of *Listeria monocytogenes* behaves not only as a riboswitch in *cis*, but also as a regulatory ncRNA in *trans* [97]. This result highlights the possibility that functional RNAs such as ribozymes and riboswitches can be responsible for performing multiple tasks. In this regard, engineering of natural ribozymes has provided additional insight.

Merging the ribozyme and riboswitch fields has created new tools to artificially control gene expression [98, 99]. Aptazymes are engineered RNAs composed of both a ligand binding domain and a ribozyme domain. They were first engineered as allosteric ribozymes *via* the fusion of an ATP aptamer and a HHR, whereby the sensing of ATP by the aptamer domain resulted in tuning of the HHR rate of catalysis [100]. The ability to adapt ribozymes into unnatural and unprecedented functional platforms attests to the versatility of these RNAs [101]. The functional flexibility of ribozymes and the dynamic range in catalytic rates makes these RNAs versatile tools in the synthetic biologist toolbox. Perhaps some of the tricks we

ask ribozymes to perform *in vitro* or *in vivo* are really characteristics that nature already uses but remain undiscovered.

Concluding Remarks

In summary, the six families of self-cleaving ribozymes described here represent some of the smallest catalytic molecules known to biology. The intricate and elegant structures unique to each ribozyme family depict different means of accomplishing the same reaction. This is useful to synthetic biology, where ribozymes can be used as platforms conveying information about ligand recognition and molecular targeting. Equally exciting and consuming is the idea that there may be many more natural RNA structures capable of catalysis that are yet to be discovered. The vast distribution for some of the ribozyme families presented here leads to many intriguing questions regarding their biological relevance.

Glossary box

Cofactor	A cofactor is a chemical compound that is directly involved in the catalytic mechanism by a catalytic macromolecule. To our knowledge, the HDV and *glmS* ribozymes are the only self-cleaving ribozyme that utilize cofactors (Mg^{2+} and glucosamine 6-phosphate, respectively) as part of their reaction mechanism.
General acid-general base catalysis	General acid/base catalysis refers to a reaction where a certain chemical group is involved in proton transfer. In most cases a nucleobase fulfills the role of general base by abstracting a proton from the 2′ OH of the attacking group and another nucleobase acts as general acid by protonating the 5′ oxyanion leaving group (Fig. 1).
Glucosamine-6-phosphate synthase (glmS)	Also known as glutamine–fructose-6-phosphate transaminase. The protein encoded by the *glmS* gene has been shown to participate in the peptidoglycan synthesis pathway for bacterial cell wall synthesis. The substrates for the aminotransferase reaction catalyzed by the glmS enzyme are L-glutamine and D-fructose 6-phosphate and the product is D-glucosamine 6-phosphate. The glmS enzyme is activated upon post-translational modifications by protein factors, and the enzyme activity is inhibited by glucose 6-phosphate.
Hepatitis Delta Virus (HDV)	The hepatitis delta virus, and HBV helper virus, has a small circular single-stranded RNA genome that codes for one protein, the delta antigen. Both the sense and antisense genomes of the virus encode a self-cleaving ribozyme of the same secondary structure, but different sequence.

Hepatitis delta virus-like (HDV-like)	The term HDV-like refers to the structural similarities between the HDV ribozyme to that of a ribozyme identified within an organism's genome. One example includes the HDV-like ribozyme encoded within the *CPEB3* gene in mammals.
Long interspersed nuclear elements (LINE)	These are a type of eukaryotic non-LTR transposon capable of propagation through an RNA intermediate. LINE elements are repetitive in sequence, can be as long as a few thousand base pairs, and encode the necessary proteins required for autonomous retrotransposition.
Long terminal repeat (LTR)	LTR refers to the repetitive sequence found at termini of a retroviral genome that encodes specific proteins necessary for infection and propagation. Non-long terminal repeats (non-LTRs) only replicate within a genome and are defined as retrotransposable elements that prime their cDNA from nicked target DNA.
Noncoding RNAs (ncRNAs)	ncRNAs are transcribed RNAs that are not translated. Many ncRNAs have been shown to participate in RNA processing and assembly in ribonucleoprotein complexes. These include tRNAs, rRNAs and small nuclear RNAs (snRNAs).
Penelope-like elements (PLEs)	PLEs are a distinct family of retrotransposons identified within a large number of eukaryotic genomes. PLEs are classified by two direct repeats flanking a single ORF (open reading frame) that encodes reverse transcriptase proteins, an endonuclease, and sometimes retains introns.
Short interspersed nuclear elements (SINE)	These are RNA fragments that are a few hundred nucleotides in length and usually are composed of tandem repeats. These RNA transcripts are not translated, but have been shown to be propagated by enzymes encoded by LINEs.
Single nucleotide polymorphism (SNP)	A SNP is a type of genetic variation that is observed within a population that shares the same genomic sequence. This variation occurs at a single nucleotide and at the same genomic location.
Transition state stabilization	A transition state is a high-energy species formed during the course of a chemical reaction. The stabilization of the transition state accelerates the chemical reaction. During ribozyme self-cleavage phosphorane forms the transition state, which can be a true intermediate if it is stabilized through hydrogen-bonding of one of the non-bridging phosphates or by a counter ion (e.g. a metal ion).
Untranslated region (UTR)	A region of an mRNA molecule that corresponds to the sequence before the translation start codon and after the translation termination codon. UTRs are important for regulation of the transcript.

Viroids	Short (~250-~450 nt) circular single-stranded RNA infectious pathogens found mostly in plants. Also known as sub-viral pathogens, they are replicated through rolling-circle replication by RNA polymerase II.
Virusoids	Similar to viroids, these are circular single-stranded RNA pathogens, but dependent on viruses for rolling-circle replication and encapsulation. They are classified as subviral particles and satellites.

References

1. Lai MM. The molecular biology of hepatitis delta virus. Annu Rev Biochem. 1995; 64:259–286. [PubMed: 7574482]
2. Taylor JM. Hepatitis delta virus. Intervirology. 1999; 42:173–178. [PubMed: 10516472]
3. Wu HN, Lin YJ, Lin FP, Makino S, Chang MF, Lai MMC. Human Hepatitis-Delta Virus-Rna Subfragments Contain an Autocleavage Activity. Proc Natl Acad Sci U S A. 1989; 86:1831–1835. [PubMed: 2648383]
4. Salehi-Ashtiani K, Luptak A, Litovchick A, Szostak JW. A genomewide search for ribozymes reveals an HDV-like sequence in the human CPEB3 gene. Science. 2006; 313:1788–1792. [PubMed: 16990549]
5. Webb CH, Riccitelli NJ, Ruminski DJ, Luptak A. Widespread occurrence of self-cleaving ribozymes. Science. 2009; 326:953. [PubMed: 19965505]
6. Ruminski DJ, Webb CH, Riccitelli NJ, Luptak A. Processing and translation initiation of non-long terminal repeat retrotransposons by hepatitis delta virus (HDV)-like self-cleaving ribozymes. Journal of Biological Chemistry. 2011; 286:41286–41295. [PubMed: 21994949]
7. Eickbush DG, Eickbush TH. R2 retrotransposons encode a self-cleaving ribozyme for processing from an rRNA cotranscript. Mol Cell Biol. 2010; 30:3142–3150. [PubMed: 20421411]
8. Sanchez-Luque FJ, Lopez MC, Macias F, Alonso C, Thomas MC. Identification of an hepatitis delta virus-like ribozyme at the mRNA 5′-end of the L1Tc retrotransposon from Trypanosoma cruzi. Nucleic Acids Res. 2011; 39:8065–8077. [PubMed: 21724615]
9. Bibillo A, Eickbush TH. The reverse transcriptase of the R2 non-LTR retrotransposon: continuous synthesis of cDNA on non-continuous RNA templates. J Mol Biol. 2002; 316:459–473. [PubMed: 11866511]
10. Bibillo A, Eickbush TH. End-to-end template jumping by the reverse transcriptase encoded by the R2 retrotransposon. Journal of Biological Chemistry. 2004; 279:14945–14953. [PubMed: 14752111]
11. Vogler C, Spalek K, Aerni A, Demougin P, Muller A, Huynh KD, de Quervain DJF. CPEB3 is associated with human episodic memory. Frontiers in Behavioral Neuroscience. 2009; 3
12. Smith JB, Dinter-Gottlieb G. Antigenomic Hepatitis delta virus ribozymes self-cleave in 18 M formamide. Nucleic Acids Res. 1991; 19:1285–1289. [PubMed: 1709487]
13. Duhamel J, Liu DM, Evilia C, Fleysh N, Dinter-Gottlieb G, Lu P. Secondary structure content of the HDV ribozyme in 95% formamide. Nucleic Acids Res. 1996; 24:3911–3917. [PubMed: 8918791]
14. Ferre-D'Amare AR, Zhou K, Doudna JA. Crystal structure of a hepatitis delta virus ribozyme. Nature. 1998; 395:567–574. [PubMed: 9783582]
15. Ke A, Zhou K, Ding F, Cate JH, Doudna JA. A conformational switch controls hepatitis delta virus ribozyme catalysis. Nature. 2004; 429:201–205. [PubMed: 15141216]
16. Chen JH, Yajima R, Chadalavada DM, Chase E, Bevilacqua PC, Golden BL. A 1.9 A crystal structure of the HDV ribozyme precleavage suggests both Lewis acid and general acid

mechanisms contribute to phosphodiester cleavage. Biochemistry. 2010; 49:6508–6518. [PubMed: 20677830]

17. Gong B, Chen JH, Bevilacqua PC, Golden BL, Carey PR. Competition between Co(NH(3)(6)3+ and inner sphere Mg2+ ions in the HDV ribozyme. Biochemistry. 2009; 48:11961–11970. [PubMed: 19888753]
18. Golden BL. Two distinct catalytic strategies in the hepatitis delta virus ribozyme cleavage reaction. Biochemistry. 2011; 50:9424–9433. [PubMed: 22003985]
19. Das SR, Piccirilli JA. General acid catalysis by the hepatitis delta virus ribozyme. Nat Chem Biol. 2005; 1:45–52. [PubMed: 16407993]
20. Thaplyal P, Ganguly A, Hammes-Schiffer S, Bevilacqua PC. Inverse Thio Effects in the Hepatitis Delta Virus Ribozyme Reveal that the Reaction Pathway Is Controlled by Metal Ion Charge Density. Biochemistry. 2015; 54:2160–2175. [PubMed: 25799319]
21. Perrotta AT, Been MD. HDV ribozyme activity in monovalent cations. Biochemistry. 2006; 45:11357–11365. [PubMed: 16981696]
22. Luptak A, Ferre-D'Amare AR, Zhou K, Zilm KW, Doudna JA. Direct pK(a) measurement of the active-site cytosine in a genomic hepatitis delta virus ribozyme. J Am Chem Soc. 2001; 123:8447–8452. [PubMed: 11525650]
23. Gong B, Chen JH, Chase E, Chadalavada DM, Yajima R, Golden BL, Carey PR. Direct measurement of a pK(a) near neutrality for the catalytic cytosine in the genomic HDV ribozyme using Raman crystallography. J Am Chem Soc. 2007; 129:13335–13342. [PubMed: 17924627]
24. Prody GA, Bakos JT, Buzayan JM, Schneider IR, Bruening G. Autolytic processing of dimeric plant virus satellite RNA. Science. 1986; 231:1577–1580. [PubMed: 17833317]
25. Forster AC, Symons RH. Self-Cleavage of Virusoid Rna Is Performed by the Proposed 55-Nucleotide Active-Site. Cell. 1987; 50:9–16. [PubMed: 3594567]
26. Forster AC, Symons RH. Self-cleavage of plus and minus RNAs of a virusoid and a structural model for the active sites. Cell. 1987; 49:211–220. [PubMed: 2436805]
27. Epstein LM, Gall JG. Transcripts of newt satellite DNA self-cleave in vitro. Cold Spring Harb Symp Quant Biol. 1987; 52:261–265. [PubMed: 3454261]
28. Rojas AA, Vazquez-Tello A, Ferbeyre G, Venanzetti F, Bachmann L, Paquin B, Cedergren R. Hammerhead-mediated processing of satellite pDo500 family transcripts from Dolichopoda cave crickets. Nucleic Acids Res. 2000; 28:4037–4043. [PubMed: 11024185]
29. Ferbeyre G, Smith JM, Cedergren R. Schistosome satellite DNA encodes active hammerhead ribozymes. Mol Cell Biol. 1998; 18:3880–3888. [PubMed: 9632772]
30. Laha T, McManus DP, Loukas A, Brindley PJ. Sjalpha elements, short interspersed element-like retroposons bearing a hammerhead ribozyme motif from the genome of the oriental blood fluke Schistosoma japonicum. Biochim Biophys Acta. 2000; 1492:477–482. [PubMed: 11004517]
31. de la Pena M, Garcia-Robles I. Ubiquitous presence of the hammerhead ribozyme motif along the tree of life. Rna. 2010; 16:1943–1950. [PubMed: 20705646]
32. de la Pena M, Garcia-Robles I. Intronic hammerhead ribozymes are ultraconserved in the human genome. EMBO Rep. 2010; 11:711–716. [PubMed: 20651741]
33. Perreault J, Weinberg Z, Roth A, Popescu O, Chartrand P, Ferbeyre G, Breaker RR. Identification of Hammerhead Ribozymes in All Domains of Life Reveals Novel Structural Variations. Plos Computational Biology. 2011; 7
34. Jimenez RM, Delwart E, Luptak A. Structure-based search reveals hammerhead ribozymes in the human microbiome. Journal of Biological Chemistry. 2011; 286:7737–7743. [PubMed: 21257745]
35. Seehafer C, Kalweit A, Steger G, Graf S, Hammann C. From alpaca to zebrafish: hammerhead ribozymes wherever you look. Rna. 2011; 17:21–26. [PubMed: 21081661]
36. Garcia-Robles I, Sanchez-Navarro J, de la Pena M. Intronic hammerhead ribozymes in mRNA biogenesis. Biol Chem. 2012; 393:1317–1326. [PubMed: 23109545]
37. Martick M, Horan LH, Noller HF, Scott WG. A discontinuous hammerhead ribozyme embedded in a mammalian messenger RNA. Nature. 2008; 454:899–U857. [PubMed: 18615019]
38. Pley HW, Flaherty KM, McKay DB. Three-dimensional structure of a hammerhead ribozyme. Nature. 1994; 372:68–74. [PubMed: 7969422]

39. Scott WG, Murray JB, Arnold JR, Stoddard BL, Klug A. Capturing the structure of a catalytic RNA intermediate: the hammerhead ribozyme. Science. 1996; 274:2065–2069. [PubMed: 8953035]
40. Khvorova A, Lescoute A, Westhof E, Jayasena SD. Sequence elements outside the hammerhead ribozyme catalytic core enable intracellular activity. Nat Struct Biol. 2003; 10:708–712. [PubMed: 12881719]
41. De la Pena M, Gago S, Flores R. Peripheral regions of natural hammerhead ribozymes greatly increase their self-cleavage activity. Embo J. 2003; 22:5561–5570. [PubMed: 14532128]
42. Martick M, Scott WG. Tertiary contacts distant from the active site prime a ribozyme for catalysis. Cell. 2006; 126:309–320. [PubMed: 16859740]
43. Ferre-D'Amare AR, Scott WG. Small self-cleaving ribozymes. Cold Spring Harb Perspect Biol. 2010; 2:a003574. [PubMed: 20843979]
44. Anderson M, Schultz EP, Martick M, Scott WG. Active-site monovalent cations revealed in a 1.55-A-resolution hammerhead ribozyme structure. J Mol Biol. 2013; 425:3790–3798. [PubMed: 23711504]
45. Han J, Burke JM. Model for general acid-base catalysis by the hammerhead ribozyme: pH-activity relationships of G8 and G12 variants at the putative active site. Biochemistry. 2005; 44:7864–7870. [PubMed: 15910000]
46. Roychowdhury-Saha M, Burke DH. Distinct reaction pathway promoted by non-divalent-metal cations in a tertiary stabilized hammerhead ribozyme. Rna. 2007; 13:841–848. [PubMed: 17456566]
47. Chi YI, Martick M, Lares M, Kim R, Scott WG, Kim SH. Capturing hammerhead ribozyme structures in action by modulating general base catalysis. Plos Biology. 2008; 6:2060–2068.
48. Martick M, Lee TS, York DM, Scott WG. Solvent structure and hammerhead ribozyme catalysis. Chem Biol. 2008; 15:332–342. [PubMed: 18420140]
49. Rubino L, Tousignant ME, Steger G, Kaper JM. Nucleotide sequence and structural analysis of two satellite RNAs associated with chicory yellow mottle virus. J Gen Virol. 1990; 71(Pt 9):1897–1903. [PubMed: 1698918]
50. Kaper JM, Tousignant ME, Steger G. Nucleotide sequence predicts circularity and self-cleavage of 300-ribonucleotide satellite of arabis mosaic virus. Biochem Biophys Res Commun. 1988; 154:318–325. [PubMed: 3395334]
51. Grum-Tokars V, Milovanovic M, Wedekind JE. Crystallization and X-ray diffraction analysis of an all-RNA U39C mutant of the minimal hairpin ribozyme. Acta Crystallogr D Biol Crystallogr. 2003; 59:142–145. [PubMed: 12499551]
52. Rupert PB, Ferre-D'Amare AR. Crystal structure of a hairpin ribozyme- inhibitor complex with implications for catalysis. Nature. 2001; 410:780–786. [PubMed: 11298439]
53. Rupert PB, Massey AP, Sigurdsson ST, Ferre-D'Amare AR. Transition state stabilization by a catalytic RNA. Science. 2002; 298:1421–1424. [PubMed: 12376595]
54. Tan E, Wilson TJ, Nahas MK, Clegg RM, Lilley DM, Ha T. A four-way junction accelerates hairpin ribozyme folding via a discrete intermediate. Proc Natl Acad Sci U S A. 2003; 100:9308–9313. [PubMed: 12883002]
55. Nahas MK, Wilson TJ, Hohng S, Jarvie K, Lilley DM, Ha T. Observation of internal cleavage and ligation reactions of a ribozyme. Nat Struct Mol Biol. 2004; 11:1107–1113. [PubMed: 15475966]
56. Kuzmin YI, Da Costa CP, Fedor MJ. Role of an active site guanine in hairpin ribozyme catalysis probed by exogenous nucleobase rescue. J Mol Biol. 2004; 340:233–251. [PubMed: 15201049]
57. Kuzmin YI, Da Costa CP, Cottrell JW, Fedor MJ. Role of an active site adenine in hairpin ribozyme catalysis. J Mol Biol. 2005; 349:989–1010. [PubMed: 15907933]
58. Wilson TJ, Ouellet J, Zhao ZY, Harusawa S, Araki L, Kurihara T, Lilley DM. Nucleobase catalysis in the hairpin ribozyme. Rna. 2006; 12:980–987. [PubMed: 16601203]
59. Pinard R, Hampel KJ, Heckman JE, Lambert D, Chan PA, Major F, Burke JM. Functional involvement of G8 in the hairpin ribozyme cleavage mechanism. Embo J. 2001; 20:6434–6442. [PubMed: 11707414]
60. Collins RA. The Neurospora Varkud satellite ribozyme. Biochem Soc Trans. 2002; 30:1122–1126. [PubMed: 12440987]

61. Bouchard P, Legault P. A remarkably stable kissing-loop interaction defines substrate recognition by the Neurospora Varkud Satellite ribozyme. Rna. 2014; 20:1451–1464. [PubMed: 25051972]
62. Beattie TL, Olive JE, Collins RA. A secondary-structure model for the self-cleaving region of Neurospora VS RNA. Proc Natl Acad Sci U S A. 1995; 92:4686–4690. [PubMed: 7753865]
63. Rastogi T, Beattie TL, Olive JE, Collins RA. A long-range pseudoknot is required for activity of the Neurospora VS ribozyme. Embo J. 1996; 15:2820–2825. [PubMed: 8654379]
64. Andersen AA, Collins RA. Rearrangement of a stable RNA secondary structure during VS ribozyme catalysis. Mol Cell. 2000; 5:469–478. [PubMed: 10882132]
65. Andersen AA, Collins RA. Intramolecular secondary structure rearrangement by the kissing interaction of the Neurospora VS ribozyme. Proc Natl Acad Sci U S A. 2001; 98:7730–7735. [PubMed: 11427714]
66. Flinders J, Dieckmann T. A pH controlled conformational switch in the cleavage site of the VS ribozyme substrate RNA. J Mol Biol. 2001; 308:665–679. [PubMed: 11350168]
67. Hiley SL, Collins RA. Rapid formation of a solvent-inaccessible core in the Neurospora Varkud satellite ribozyme. Embo J. 2001; 20:5461–5469. [PubMed: 11574478]
68. Hiley SL, Sood VD, Fan J, Collins RA. 4-thio-U cross-linking identifies the active site of the VS ribozyme. Embo J. 2002; 21:4691–4698. [PubMed: 12198171]
69. Bouchard P, Legault P. Structural insights into substrate recognition by the Neurospora Varkud satellite ribozyme: importance of U-turns at the kissing-loop junction. Biochemistry. 2014; 53:258–269. [PubMed: 24325625]
70. Michiels PJA, Schouten CHJ, Hilbers CW, Heus HA. Structure of the ribozyme substrate hairpin of Neurospora VS RNA: A close look at the cleavage site. Rna-a Publication of the Rna Society. 2000; 6:1821–1832.
71. Hoffmann B, Mitchell GT, Gendron P, Major F, Andersen AA, Collins RA, Legault P. NMR structure of the active conformation of the Varkud satellite ribozyme cleavage site. Proc Natl Acad Sci U S A. 2003; 100:7003–7008. [PubMed: 12782785]
72. Lipfert J, Ouellet J, Norman DG, Doniach S, Lilley DM. The complete VS ribozyme in solution studied by small-angle X-ray scattering. Structure. 2008; 16:1357–1367. [PubMed: 18786398]
73. Wilson TJ, McLeod AC, Lilley DM. A guanine nucleobase important for catalysis by the VS ribozyme. Embo J. 2007; 26:2489–2500. [PubMed: 17464286]
74. Wilson TJ, Li NS, Lu J, Frederiksen JK, Piccirilli JA, Lilley DM. Nucleobase-mediated general acid-base catalysis in the Varkud satellite ribozyme. Proc Natl Acad Sci U S A. 2010; 107:11751–11756. [PubMed: 20547881]
75. Winkler WC, Nahvi A, Roth A, Collins JA, Breaker RR. Control of gene expression by a natural metabolite-responsive ribozyme. Nature. 2004; 428:281–286. [PubMed: 15029187]
76. McCarthy TJ, Plog MA, Floy SA, Jansen JA, Soukup JK, Soukup GA. Ligand requirements for glmS ribozyme self-cleavage. Chem Biol. 2005; 12:1221–1226. [PubMed: 16298301]
77. Roth A, Nahvi A, Lee M, Jona I, Breaker RR. Characteristics of the glmS ribozyme suggest only structural roles for divalent metal ions. Rna. 2006; 12:607–619. [PubMed: 16484375]
78. Klein DJ, Ferre-D'Amare AR. Structural basis of glmS ribozyme activation by glucosamine-6-phosphate. Science. 2006; 313:1752–1756. [PubMed: 16990543]
79. Cochrane JC, Lipchock SV, Strobel SA. Structural investigation of the glmS ribozyme bound to Its catalytic cofactor. Chem Biol. 2007; 14:97–105. [PubMed: 17196404]
80. Cochrane JC, Lipchock SV, Smith KD, Strobel SA. Structural and chemical basis for glucosamine 6-phosphate binding and activation of the glmS ribozyme. Biochemistry. 2009; 48:3239–3246. [PubMed: 19228039]
81. Gong B, Klein DJ, Ferre-D'Amare AR, Carey PR. The glmS Ribozyme Tunes the Catalytically Critical pK(a) of Its Coenzyme Glucosamine-6-phosphate. J Am Chem Soc. 2011; 133:14188–14191. [PubMed: 21848325]
82. Viladoms J, Fedor MJ. The glmS Ribozyme Cofactor is a General Acid-Base Catalyst. J Am Chem Soc. 2012; 134:19043–19049. [PubMed: 23113700]

83. Roth A, Weinberg Z, Chen AGY, Kim PB, Ames TD, Breaker RR. A widespread self-cleaving ribozyme class is revealed by bioinformatics. Nat Chem Biol. 2014; 10:56–U92. [PubMed: 24240507]
84. Liu Y, Wilson TJ, McPhee SA, Lilley DM. Crystal structure and mechanistic investigation of the twister ribozyme. Nat Chem Biol. 2014; 10:739–744. [PubMed: 25038788]
85. Ren AM, Kosutic M, Rajashankar KR, Frener M, Santner T, Westhof E, Patel DJ. In-line alignment and Mg2+ coordination at the cleavage site of the env22 twister ribozyme. Nature Communications. 2014; 5
86. Eiler D, Wang J, Steitz TA. Structural basis for the fast self-cleavage reaction catalyzed by the twister ribozyme. Proc Natl Acad Sci U S A. 2014; 111:13028–13033. [PubMed: 25157168]
87. Pyle AM. Ribozymes: a distinct class of metalloenzymes. Science. 1993; 261:709–714. [PubMed: 7688142]
88. Yarus M. How many catalytic RNAs? Ions and the Cheshire cat conjecture. Faseb J. 1993; 7:31–39. [PubMed: 8422972]
89. Salehi-Ashtiani K, Szostak JW. In vitro evolution suggests multiple origins for the hammerhead ribozyme. Nature. 2001; 414:82–84. [PubMed: 11689947]
90. Fong N, Ohman M, Bentley DL. Fast ribozyme cleavage releases transcripts from RNA polymerase II and aborts co-transcriptional pre-mRNA processing. Nat Struct Mol Biol. 2009; 16:916–922. [PubMed: 19701200]
91. Lacadie SA, Tardiff DF, Kadener S, Rosbash M. In vivo commitment to yeast cotranscriptional splicing is sensitive to transcription elongation mutants. Genes Dev. 2006; 20:2055–2066. [PubMed: 16882983]
92. Cervera A, De la Pena M. Eukaryotic penelope-like retroelements encode hammerhead ribozyme motifs. Mol Biol Evol. 2014; 31:2941–2947. [PubMed: 25135949]
93. Forster AC, Davies C, Sheldon CC, Jeffries AC, Symons RH. Self- Cleaving Viroid and Newt Rnas May Only Be Active as Dimers. Nature. 1988; 334:265–267. [PubMed: 2456468]
94. Hammann C, Luptak A, Perreault J, de la Pena M. The ubiquitous hammerhead ribozyme. Rna. 2012; 18:871–885. [PubMed: 22454536]
95. Weinberg Z, Kim PB, Chen TH, Li S, Harris KA, Lunse CE, Breaker RR. New classes of self-cleaving ribozymes revealed by comparative genomics analysis. Nat Chem Biol. 2015; 11:606–610. [PubMed: 26167874]
96. Tang J, Breaker RR. Structural diversity of self-cleaving ribozymes. Proc Natl Acad Sci U S A. 2000; 97:5784–5789. [PubMed: 10823936]
97. Loh E, Dussurget O, Gripenland J, Vaitkevicius K, Tiensuu T, Mandin P, Johansson J. A trans-acting riboswitch controls expression of the virulence regulator PrfA in Listeria monocytogenes. Cell. 2009; 139:770–779. [PubMed: 19914169]
98. Vinkenborg JL, Karnowski N, Famulok M. Aptamers for allosteric regulation. Nat Chem Biol. 2011; 7:519–527. [PubMed: 21769099]
99. Famulok M, Hartig JS, Mayer G. Functional aptamers and aptazymes in biotechnology, diagnostics, and therapy. Chem Rev. 2007; 107:3715–3743. [PubMed: 17715981]
100. Tang J, Breaker RR. Rational design of allosteric ribozymes. Chem Biol. 1997; 4:453–459. [PubMed: 9224568]
101. Carothers JM, Goler JA, Juminaga D, Keasling JD. Model-driven engineering of RNA devices to quantitatively program gene expression. Science. 2011; 334:1716–1719. [PubMed: 22194579]
102. Riccitelli NJ, Luptak A. Computational discovery of folded RNA domains in genomes and in vitro selected libraries. Methods. 2010; 52:133–140. [PubMed: 20554049]

Box 1. Structural conservation in ribozymes

As a single-stranded nucleic acid polymer, RNA is capable of folding into diverse and intricate secondary and tertiary structures. The basis of RNA secondary structure is its capacity for base-pairing of antiparallel strands into helices within a single molecule. Since base-pairing only dictates that complementary nucleotides are recognized through standard Watson-Crick or wobble interactions, the actual sequence of a helix need not be conserved, as long as the interacting nucleotides are complementary (e.g. within a helix a C-G base-pair serves the same function as an A-U). In general, structures of RNAs are dominated by helical segments, which are defined on the sequence level by base-pair co-variation. Unlike protein structures, which typically share conserved sequences, RNA motifs are therefore typically not conserved on sequence level, but are dominated by segments of sequence that co-vary with their pairing partners and are thus hard to identify through sequence alignments. Currently, bioinformatics methods identify patterns of covariation across predicted secondary structures, and these patterns are an indicator of RNA structural conservation, leading to the discovery of new functional RNA families [102].

Tertiary structure is the global architecture of a single molecule formed by the combination of contacts outside of helical base-pairing through hydrogen bonding, base-stacking, and other specific interactions. An RNA structural motif is conserved if it preserves the secondary and tertiary structure, although not necessarily the topology, of an RNA. Here topology refers to the order that the individual structural elements appear in the motif. For example the Y-shaped hammearhead ribozyme (Fig. 3B) can connect to the flanking transcript *via* the termini of any of its three helices, giving rise to three different topologies, but the same tertiary structure.

Outstanding Questions Box

- What are the mechanisms of transition-state (or intermediate) stabilization during ribozyme catalysis for all known self-cleaving ribozymes?
- What are the strategies to shift pK_as of active site groups involved in catalysis?
- Are there natural *trans*-cleaving ribozymes?
- Are there natural aptazymes?
- What are the effects of mammalian self-cleaving ribozymes on their hosts?

Trends Box

-Self-cleaving ribozymes are distributed throughout all branches of life. Currently there are nine distinct structural motifs that promote self-scission in nature.

-The six self-cleaving ribozymes that have been investigated mechanistically all appear to use general acid-base mechanism for catalysis. Magnesium, or another divalent metal ion, is largely used to stabilize the tertiary structures of these ribozymes.

-The broad distribution of self-cleaving ribozymes suggests several biological roles. The known functions include RNA processing during rolling-circle replication of single-stranded subviral pathogens and satellites, co-transcriptional scission of retrotransposons, and (pre-)mRNA cleavage.

-Genomic locations of these ribozymes suggest that they may affect many other biological processes, some of which may not be directly associated with RNA scission.

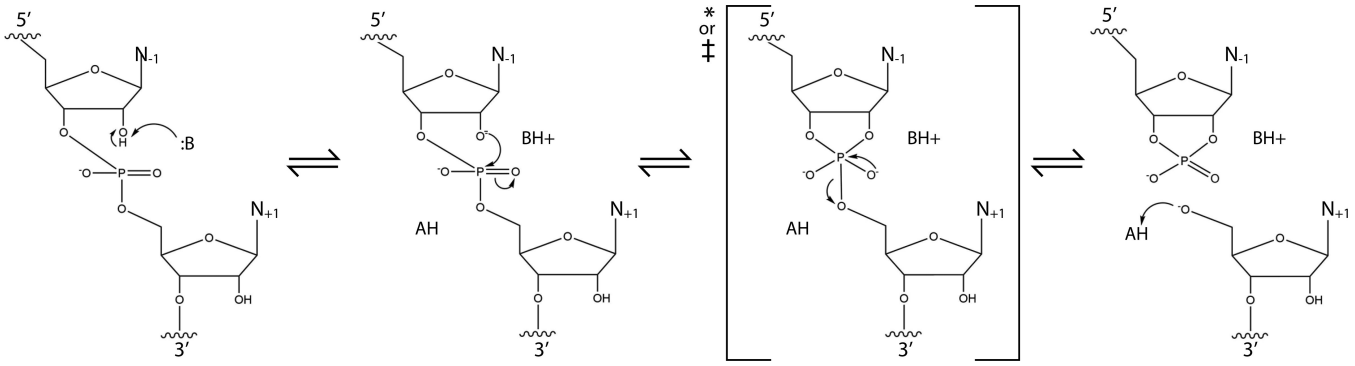

Figure 1. Mechanism of RNA self-scission

A general acid-base catalysis involves a general base, which deprotonates the 2′ hydroxyl of the nucleophile, positioned in-line with the 5′ O leaving group. The transesterification proceeds *via* a phosphorane transition state or intermediate, depending on whether it is stabilized, yielding a 2′-3′ cyclic phosphate in the upstream nucleotide and an oxyanion on the downstream nucleotide. The leaving group is protonated by a general base. The small self-cleaving ribozymes described here use a variety of chemical groups to facilitate this process (Table 1).

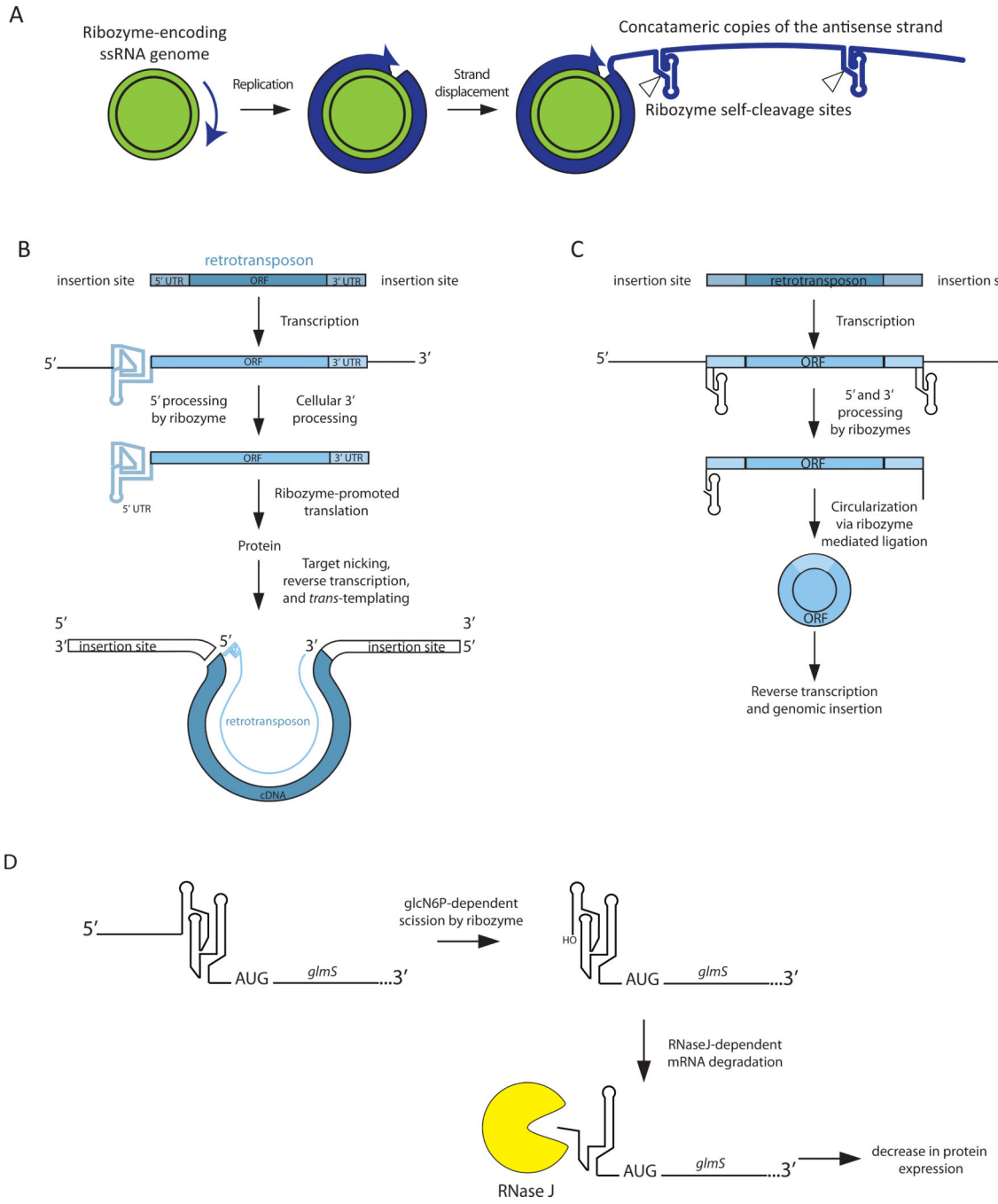

Figure 2. Roles of self-cleaving ribozymes in different biological systems

(A) Most instances of self-cleaving ribozymes found in (sub-)viral genomes are involved in replication. During rolling-circle replication of a single-stranded RNA genome, concatameric copies of the opposite polarity are generated. The self-cleavage activity of ribozymes generates unit-length copies that must be circularized and replicated to complete the cycle. (B) Retrotransposon-associated hepatitis delta virus HDV-like ribozymes liberate the 5′ end of the retroelement from the full-length transcript. The ribozyme structure in the 5′ UTR promotes translation of the downstream ORF. The protein produced is necessary for

target nicking, reverse transcription, and genomic insertion. Further, the HDV-like ribozyme on the 5′ end of the RNA promotes the template switching necessary to complete genomic insertion of the autonomous (LINE) element. (C) Hammerhead ribozymes mapping to non-autonomous retrotransposons (SINEs) serve to mobilize the retroelement. Complementarity of the 5′ and 3′ ends facilitates ribozyme self-ligation resulting in circularization of the RNA; this feature enhances the reverse transcription and genomic insertion processes that complete the retrotransposition cycle. (D) The *glmS* ribozyme is located in the 5′ UTR of the *glmS* gene, encoding the glutamine-fructose 6-phosphate aminotransferase enzyme responsible for generating glucosamine 6-phosphate (glcN6P), necessary for bacterial cell wall synthesis. The ribozyme requires glcN6P as a cofactor for catalysis. The resulting 5′-hydroxyl makes the processed transcript a substrate for the 5′-3′ exonuclease RNase J. Therefore, the *glmS* ribozyme is a riboswitch that turns off glcN6P synthase expression in response to glcN6P.

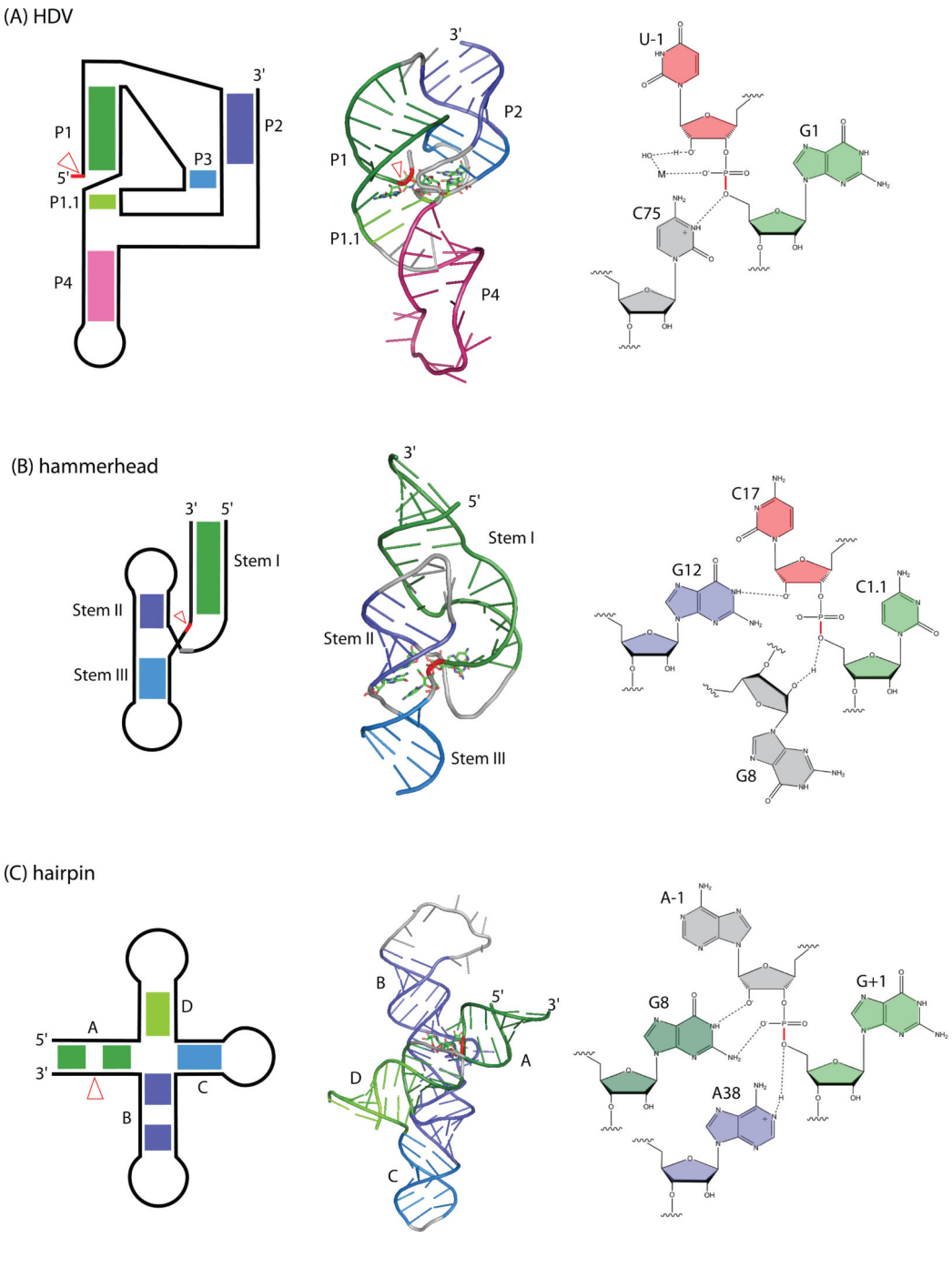

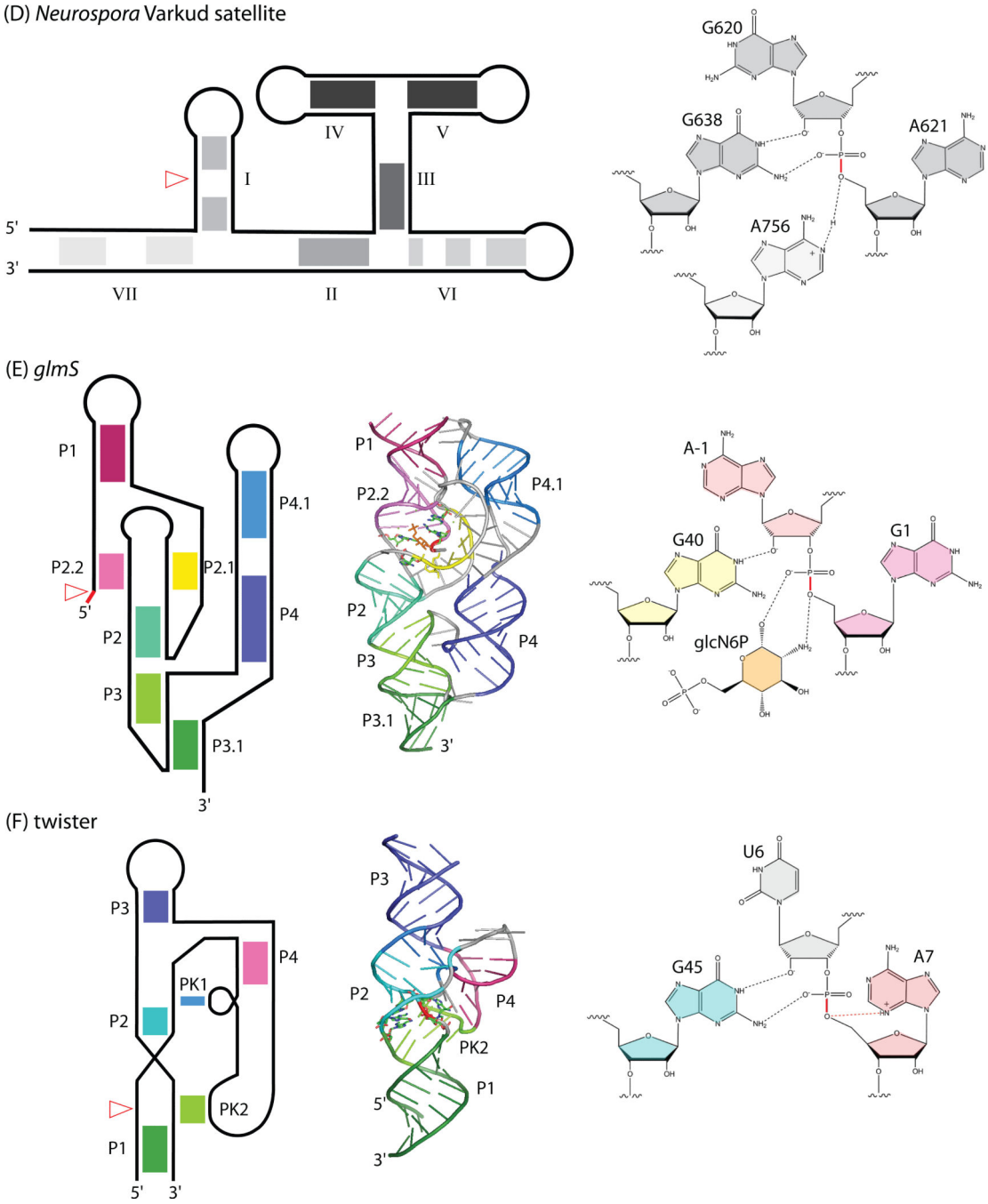

Figure 3. Overview of self-cleaving ribozymes: structural features and proposed cleavage mechanisms

The secondary structures of the (A) HDV-like, (B) hammerhead, (C) hairpin, (D) *Neurospora* Varkud satellite, (E) *glmS*, and (F) twister ribozymes are shown in the left column and labeled as they appear in current literature. Typically, the helical segments are numbered as “paired” elements (P1, P2, etc), by Roman numerals, or in alphabetical order in 5′ to 3′ direction as they appear in the first example of a given motif. Paired regions corresponding to pseudoknots are designated PK or simply as paired elements. The corresponding crystal structures for each ribozyme are shown in the middle column with

colored helices to emphasize helical stacks and pseudoknots. The site of scission is pointed out by the red arrowheads in the secondary structures and highlighted in red in the respective crystal structures. A model of the cleavage site for each ribozyme is shown in the right column, which illustrates interactions that promote the cleavage event. Nucleobases flanking the scissile phosphate are splayed apart, which promotes the in-line orientation necessary to accomplish cleavage. The scissile bond is shown in red. Interactions proposed to stabilize the transition state of the reaction are shown for all ribozymes. Note that all cleavage sites, with the exception of the HDV-like ribozyme, which requires a hydrated metal (M), have a guanosine residue that participates as a proposed general base in the general acid-base reaction mechanism. The *glmS* ribozyme requires glucosamine 6-phosphate (glcN6P) as a cofactor necessary for catalysis. For the twister ribozyme, a hypothetical interaction (dashed red line) between N3 of A_7 and the scissile phosphate suggests that A_7 may act as the general acid during self-cleavage.

PDBIDs: 3ZD5, ISJ3, IM5K, 2NZ4, 4QJH

Table 1

Common themes in self-cleavage mechanisms.

Ribozyme family	Deprotonates 2′ nucleophile	Proposed transition state stabilization	Protonates 5′ leaving group
HDV	hydrated Mg^{2+} [14, 16]	Mg^{2+} as Lewis acid	C_{75}
Hammerhead	G_{12} [43]	?	G_8
Hairpin	G_8 [52]	G_8	A_{38}
Neurospora VS	G_{638} [60]	G_{638}	A_{756}
glmS	G_{40} [78, 79]	glcN6P	glcN6P
Twister (Osa-1-4) (*env22*) (env)	G_{45} [84-86] C_{46}, **A_{47}**? [60] G_{62} [84-86]	G_{45} A_{47}, **G_{48}** A_{63}	A_7? ? ?